Journal of Thermal Engineering, Vol. 3 No. 5, pp. 1478-1488, October, 2017
Yildiz Technical University Press, Istanbul, Turkey

APPLICATION OF A NOVEL THERMO-ECOLOGICAL PERFORMANCE CRITERION: EFFECTIVE ECOLOGICAL POWER DENSITY (EFECPOD) TO A JOULE-BRAYTON CYCLE (JBC) TURBINE

G. Gonca[1,*]

ABSTRACT
This study presents an application of a new performance analysis criterion named as Effective Ecological Power Density (EFECPOD) to a Joule-Brayton cycle (JBC) turbine. The turbine performance is expressed a single value by the proposed criterion using effective efficiency, effective power, cycle temperature ratio and volume. NOx formation and turbine dimensions are considered by the cycle temperature ratio and turbine volume, respectively. The turbine volume is also related to production cost of the heat engine. Therefore, the proposed criterion is essential for multi purpose optimization. Furthermore, this criterion can be developed and applied to the other gas cycle and heat engines. Also, the influences of engine design parameters such as cycle temperature ratio, pressure ratio, turbine speed, and equivalence ratio on the EFECPOD have been examined based on Finite-Time Thermodynamics Modelling (FTTM). In order to obtain realistic results, temperature-dependent specific heats for working fluid have been used and heat transfer and exhaust output losses have been taken into consideration. The results presented could be an essential tool for JBC turbine designers.

Keywords: *Joule-Brayton Cycle, Thermodynamic Analysis, Performance Optimization, Gas Turbine*

INTRODUCTION
Gas turbines are used in so many places such as ships, tanks, air planes, power plants etc. in order to provide mechanical energy and electrical energy. In the literature so many studies have been done about the gas turbines and their cycle named as Joule-Brayton cycle.

Zare et al. [1] conducted an exergoeconomic investigation on a combined cycle in which the waste heat from the Gas Turbine-Modular Helium Reactor (GT-MHR) is recovered by an ammonia–water power/cooling cogeneration system using parametric analyses. They claimed that the unit cost of products was decreased by 5.4% by combining these two cycles. However, total investment cost rate increased just about 1%. Singh et al. [2] proposed a performance scheme for Extremum-seeking control of a supercritical carbon-dioxide closed Brayton cycle coupled with solar thermal power plant. Singh et al. [3] examined the Dynamic characteristics of a direct-heated supercritical closed Brayton power conversion system with carbon-dioxide in a solar thermal power plant. Abd El-Maksoud [4] increased the performance of a gas turbine by combining isothermal concept and binary Brayton cycle. They proposed this combination for future power generation. Singh et al. [5] examined the effect of the relative volume-ratios on dynamic characteristics of a closed Brayton cycle with supercritical carbon-dioxide in a solar-thermal power plant. Ferraro et al. [6] thermodynamically analyzed the performance of solar plants running with cylindrical parabolic collectors and air turbine engines in an open Joule–Brayton cycle using an improved model. Haseli [7] carried out an optimization study for a regenerative Brayton cycle by maximization of second law efficiency. Plaznik et al. [8] theoretically and experimentally analyzed the effects of different magnetic thermodynamic cycles such as Brayton, Ericsson and Hybrid Brayton–Ericsson cycles on the performance of a magnetic cooling device with an active magnetic regenerator. Malinowski and Lewandowska [9] presented a universal analytical model based on the Brayton cycle for part-load operation of gas microturbines to analyze energetic and exergetic efficiencies. Sim et al. [10] developed a micro-power pack using automotive alternators powered by a micro-gas turbine based on simple Brayton cycle to recharge battery packs of electric vehicles. Rao and Francuz [11] provided an identification and assessment for advanced performance improvements of combined cycles in coal based power systems. Ablay [12] proposed a new modeling approach and load following control strategy for gas turbine nuclear power plants so as to assess a way for concept designs. They presented computational results to prove the validity and effectiveness of the proposed

This paper was recommended for publication in revised form by Regional Editor Derya Burcu Özkan
[1]Department of Naval Architecture and Marine Engineering, Yildiz Technical University, Istanbul, TURKEY
**E-mail address: ggonca@yildiz.edu.tr*
Manuscript Received 22 January 2016, Accepted 29 September 2016

modeling. Mahto and Pal [13] performed thermodynamic and thermo-economic analysis of simple combined cycle power plant with gas turbine blade cooling by means of fogging. Fernández-Villacé and Paniagua [14] developed a methodology to evaluate exergetic effectiveness, propulsive efficiency, total loss and subcomponent losses of a combined cycle engine. Pantaleo et al. [15] proposed a thermo-economic assessment of a small scale micro-gas turbine fuelled with solid biomass and natural gas in Italy. Singh and Kaushik [16] presented an evaluation and thermoeconomic optimization for a Brayton–Rankine–Kalina combined triple power cycle using Specific Exergy Costing methodology. Goodarzi et al. [17] modified regenerative Brayton and inverse Brayton cycle partially by passing the airflow entering the regenerator. The results showed that higher power output with reasonable thermal efficiency can be generated by adjusting the bypass mass flow ratio. Al-Sulaiman and Atif [18] thermodynamically performed a comparison study for different supercritical carbon dioxide Brayton cycles integrated with a solar power tower. Le Roux et al. [19] defined the first law and second law efficiencies of a stainless steel closed-tube open rectangular cavity solar receiver for a small-scale solar thermal Brayton cycle. Dutta et al. [20] proposed a solid sorption based Brayton cycle using R134a, CO2, R507a, propane, R32 and R410a with activated carbon as sorbent.

This study reports a new performance analysis criterion named as EFECPOD includes the effective efficiency, effective power, cycle temperature ratio and turbine volume. In the literature, there is not any criterion covers effective efficiency, effective power, maximum combustion temperatures and turbine dimensions altogether, based on finite time thermodynamics. Furthermore, a comprehensive comparison for the design parameters such as pressure ratio, turbine speed, turbine diameter, turbine length, heat transfer coefficient, equivalence ratio has been presented. The results could be used by real turbine designers to optimize the JBC gas turbines in terms of dimensions, performance and NOx emissions.

THEORETICAL MODEL

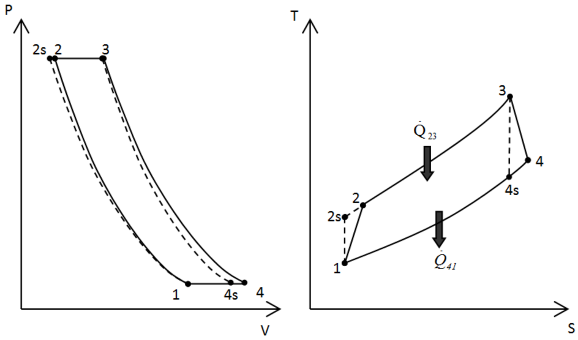

Figure 1. P-v diagram for the irreversible Diesel-Miller cycle

This study presents a comprehensive analysis for JBC which is depicted in Figure 1. A numerical simulation of EFECPOD is carried out based on FTTM. In the analysis, pressure ratio (λ), residual gas fraction (RGF), turbine speed (N), inlet temperature (T_1), inlet pressure (P_1), combustion chamber wall temperature (T_W), mass flow rate of the air ($\dot{m}$), heat transfer coefficient (h_{tr}), turbine bore (b) and length (L) are defined as follow; 4, 5%, 3000 rpm, 300 K, 100 kPa, 400 K, 1 kW/m2K, 0.5 m, 1 respectively, at the standard conditions.

In the present model, the evaluated criteria called effective ecological power density, effective power and effective efficiency could be stated as follow:

$$EFECPOD = \frac{\eta_{ef} P_{ef}}{\frac{T_1}{T_0}\alpha V_T}, P_{ef} = \dot{Q}_{in} - \dot{Q}_{out}, \eta_{ef} = \frac{P_{ef}}{\dot{Q}_f} \tag{1}$$

Where, the total heat addition $\left(\dot{Q}_{in}\right)$ at constant pressure (2-3) and the total heat rejection $\left(\dot{Q}_{out}\right)$ at constant volume (4-1) could be written as below:

$$\dot{Q}_{in} = \dot{Q}_{f,c} - \dot{Q}_{ht} = \dot{m}_T \left[\int_{T_2}^{T_3} C_p dT\right] \tag{2}$$

$$\dot{Q}_{out} = \dot{m}_T \left[\int_{T_1}^{T_4} C_P dT \right] \tag{3}$$

Where T_0 and T_1 are the ambient temperature and the temperature at the beginning of the compression. α is cycle temperature ratio and it is stated as below:

$$\alpha = \frac{T_{max}}{T_{min}} = \frac{T_4}{T_1} \tag{4}$$

Where η_c is isentropic efficiency for the compression process, λ is pressure ratio and it may be expressed as:

$$\lambda = P_2 / P_1 \tag{5}$$

Where $\dot{Q}_f$ is the total heat potential of the injected fuel and it is given as below:

$$\dot{Q}_f = \dot{m}_f H_u \tag{6}$$

Where H_u is lower heat value (LHV). $\dot{m}_f$ is time-dependent fuel mass and it can be expressed as follows:

$$\dot{m}_f = \frac{m_f N}{60} \tag{7}$$

Where $\dot{m}_f$ is fuel mass per cycle (kg). $\dot{Q}_{f,c}$ is heat released by combustion; $\dot{Q}_{ht}$ is the heat loss by heat transfer into cylinder wall and they are given as below:

$$\dot{Q}_{f,c} = \eta_c \dot{m}_f H_u \tag{8}$$

$$\dot{Q}_{ht} = h_{tr} A_{sur} (T_{me} - T_W) = h_{tr} A_{sur} (\frac{T_2 + T_3}{2} - T_W) \tag{9}$$

Where, η_c is combustion efficiency. It can be written as below [21-24]:

$$\eta_c = -1,44738 + 4,18581/\phi - 1,86876/\phi^2 \tag{10}$$

ϕ is equivalence ratio and it can be written as below:

$$\phi = \frac{\left(m_f / m_a\right)}{F_{st}} \tag{11}$$

Where, m_a is air mass per cycle (kg), V_T is total turbine volume, A_{sur} is surface area where heat transfer is carried out, F_{st} is stoichiometric fuel-air ratio [25] and they are given as follow:

$$m_a = \rho_a \mathrm{V}_a = \rho_a \left(\mathrm{V}_T - \mathrm{V}_{rg}\right) \tag{12}$$

$$\mathrm{V}_T = \mathrm{V}_{\max} = m_T v_4 = \frac{\pi b^2 L}{4} \tag{13}$$

$$A_{sur} = \frac{4\mathrm{V}_T}{b} \tag{14}$$

$$F_{st} = \frac{\varepsilon \cdot (12.01 \cdot \alpha + 1.008 \cdot \beta + 16 \cdot \gamma + 14.01 \cdot \delta)}{28.85} \tag{15}$$

Where b and L are turbine bore (inner diameter) and turbine length, v_4 is specific volume of the state point 4 in which the specific volume of cycle is the maximum. m_T is the total mass of the working fluid and it can be expresses as follows:

$$m_T = m_a + m_f + m_{rg} \tag{16}$$

Where m_{rg} is mass residual gas (kg) per cycle, which is given as:

$$m_{rg} = \rho_{rg} \mathrm{V}_{rg} \tag{17}$$

Where ρ_a and ρ_{rg} are the densities of the air and residual gas in the turbine, they can be obtained from functions below:

$$\rho_a = f(T_1, P_1) \tag{18}$$

$$\rho_{rg} = f(T_{mix}, P_1) \tag{19}$$

Where T_{mix} is average temperature of air-steam mixture. They are given as below:

$$T_{mix} = \frac{\dot{m}_a T_1 R_a + \dot{m}_{rg} T_1 R_{rg}}{\dot{m}_a R_a + \dot{m}_{rg} R_{rg}} \tag{20}$$

R_a and R_{rg} are gas constants of air and residual gas. Their values are taken as 0.287 kJ/kg.K

The compression ratio (r) is given as:

$$r = V_1 / V_2 \tag{21}$$

Time-dependent values of m_a and m_{rg} can be attained as below:

$$\dot{m}_a = \frac{m_a N}{60} = \frac{\dot{m}_f F_{st}}{\phi} \tag{22}$$

$$\dot{m}_{rg} = \frac{m_{rg} N}{60} = \dot{m}_a RGF \tag{23}$$

Where N and RGF are the turbine speed and the residual gas fraction, V_a and V_{rg} are volumes of air and residual gas, f stands for function. The functional expressions are obtained by using EES software [26] Where subscript "1" stands for the condition before the compression process (state point 1). T_1 and P_1 are in-cylinder temperature and pressure at the beginning of compression process. The fuel used in the model is octane and its chemical formula is given as C_8H_{18} [25].

Where $\alpha, \beta, \gamma, \delta$ are atomic numbers of carbon, hydrogen, oxygen, nitrogen in fuel, respectively. ε is molar fuel-air ratio [25]:

$$\varepsilon = \frac{0,21}{\left(\alpha - \frac{\gamma}{2} + \frac{\beta}{4}\right)} \tag{24}$$

Where T_{me} and T_W are mean combustion temperature and cylinder wall temperature. C_P and C_V are constant pressure and constant volume specific heats, they could be written for the temperature range of 300-3500 K as below [27]:

$$\begin{aligned} C_P &= 2.506 \cdot 10^{-11} T^2 + 1.454 \cdot 10^{-7} T^{1.5} - 4.246 \cdot 10^{-7} T + 3.162 \cdot 10^{-5} T^{0.5} \\ &+ 1.3301 - 1.512 \cdot 10^4 T^{-1.5} + 3.063 \cdot 10^5 T^{-2} - 2.212 \cdot 10^7 T^{-3} \end{aligned} \tag{25}$$

$$C_V = C_P - R \tag{26}$$

The equations for reversible adiabatic processes (1-2s) and (3-4s) are respectively as follows:

$$C_{V_1} \cdot \ln\left|\frac{T_{2s}}{T_1}\right| = R \ln|r| \quad , C_{V_2} \cdot \ln\left|\frac{T_{4s}}{T_3}\right| = R \cdot \ln\left|\frac{1}{r}\right| \tag{27}$$

Where,

$$\begin{aligned} C_{V_1} &= 2.506 \cdot 10^{-11} T_{2s1}{}^2 + 1.454 \cdot 10^{-7} T_{2s1}{}^{1.5} - 4.246 \cdot 10^{-7} T_{2s1} + 3.162 \cdot 10^{-5} T_{2s1}{}^{0.5} + \\ &1.0433 - 1.512 \cdot 10^4 T_{2s1}{}^{-1.5} + 3.063 \cdot 10^5 T_{2s1}{}^{-2} - 2.212 \cdot 10^7 T_{2s1}{}^{-3} \end{aligned} \tag{28}$$

$$\begin{aligned} C_{V_2} &= 2.506 \cdot 10^{-11} T_{4s3}{}^2 + 1.454 \cdot 10^{-7} T_{4s3}{}^{1.5} - 4.246 \cdot 10^{-7} T_{4s3} + 3.162 \cdot 10^{-5} T_{4s3}{}^{0.5} + \\ &1.0433 - 1.512 \cdot 10^4 T_{4s3}{}^{-1.5} + 3.063 \cdot 10^5 T_{4s3}{}^{-2} - 2.212 \cdot 10^7 T_{4s3}{}^{-3} \end{aligned} \tag{29}$$

$$T_{2s1} = \frac{T_{2s} - T_1}{\ln \frac{T_{2s}}{T_1}}, T_{4s1} = \frac{T_{4s} - T_3}{\ln \frac{T_{4s}}{T_3}} \tag{30}$$

$$\beta = P_3 / P_2 = T_3 / T_2 \tag{31}$$

β is named as pressure ratio. For irreversible conditions, T_2 and T_4 could be written as below:

$$T_2 = \frac{T_{2S} + T_1(\eta_C - 1)}{\eta_C} \tag{32}$$

$$T_4 = T_4 + \eta_E (T_{4S} - T_3) \tag{33}$$

Where η_C and η_E are isentropic efficiencies for the compression and expansion processes, respectively.

RESULTS AND DISCUSSION

In this study, a new performance anlysis criterion named as EFECPOD and FTTM have been applied to a JBC gas turbine.

Figure 2 show the effects of pressure ratio on the EFECPOD with respect to equivalence ratio. There are optimum points of the equivalence ratio for the EFECPOD at the constant turbine speed and air mass flow rate. The equivalence ratios give the maximum EFECPOD and effective efficiency increase to a particular value and then start to decrease with increasing equivalence ratio. The maximum values of EE and EFECPOD increase with increasing pressure ratio owing to high temperatures and pressures in the combustion chamber. Also, the turbine volume decreases with increasing pressure ratio to provide constant air mass flow rate and turbine speed. Therefore, higher performance can be obtained at the lower turbine volume.

Figures 3 and 4 show the influence of turbine speed on the EE and EFECPOD for constant pressure ratio-air mass per cycle and constant pressure ratio-mass flow rate of the air introduced into the compressor. Total intake air and injected fuel per second enhance with increasing engine speed, therefore, turbine performance increases at the constant cycle air mass conditions. At this condition, the EE and EFECPOD increase since the turbine volume and maximum combustion temperatures increase with increasing turbine speed. However, the turbine volume which is needed to provide constant air mass flow rate abates with increasing turbine speed.

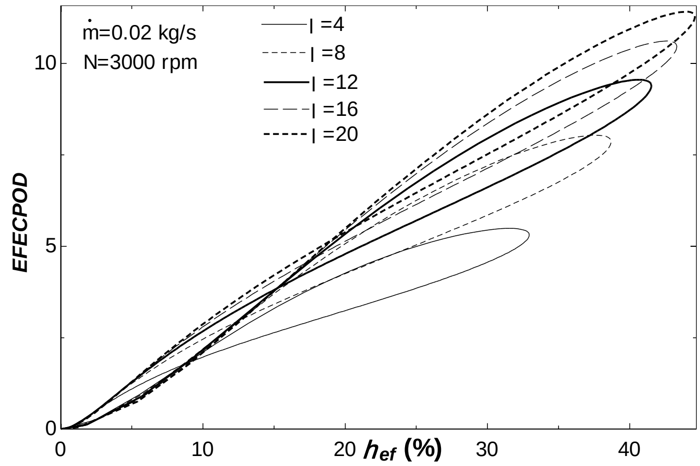

Figure 2. The variation of $EFECPOD$ with respect to η_{ef} at constant N and $\dot{m}$ for different pressure ratios

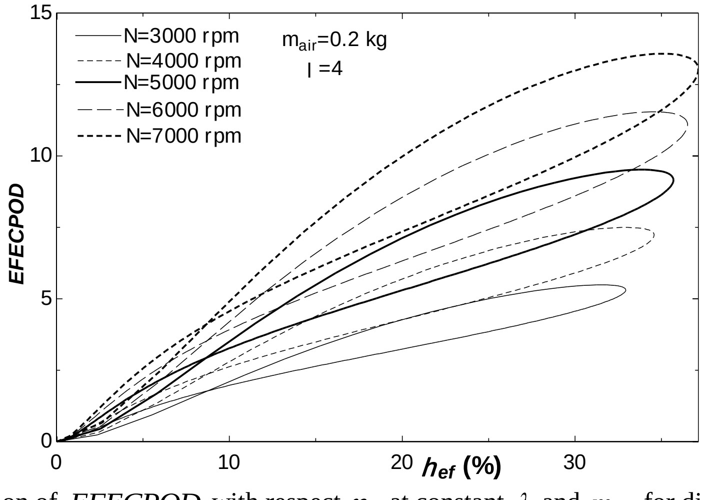

Figure 3. The variation of $EFECPOD$ with respect η_{ef} at constant λ and m_{air} for different turbine speed

Figures 5-6 illustrate the effects of turbine diameter and length on the turbine performance at constant mass flow rate and pressure ratio. While the increase of turbine diameter provides performance increment between 0.5-2.5 m, increase of turbine length leads to a reduction in the performance parameters between 1-5 m. Although both of the length and diameter are related to turbine dimensions, their changes affect the performance reversely, since the heat transfer area decreases with the diameter increment and the length reduction. Increasing heat transfer area causes to performance retrogression as higher heat transfer loss is occurred.

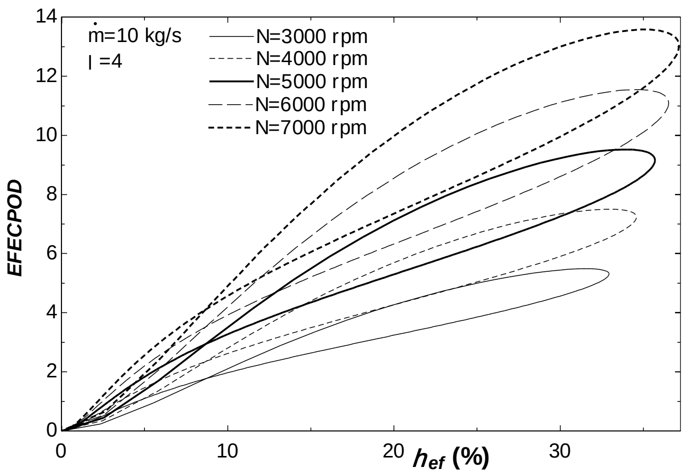

Figure 4. The variation of $EFECPOD$ with respect η_{ef} at constant λ and $\dot{m}$ for different turbine speed

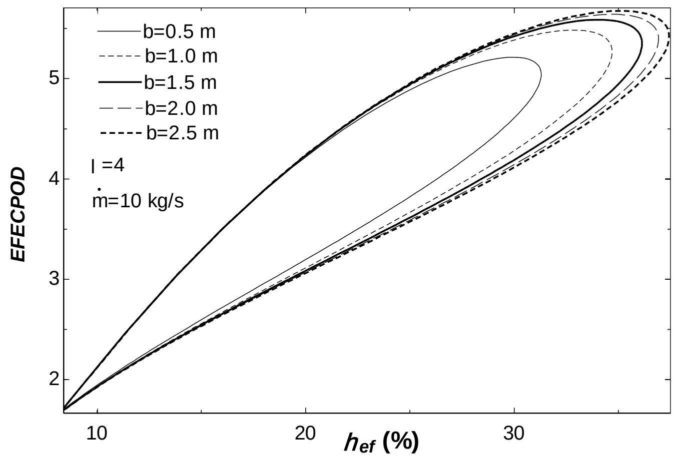

Figure 5. The variation of $EFECPOD$ with respect to η_{ef} , at constant λ and $\dot{m}$ for different turbine diameter

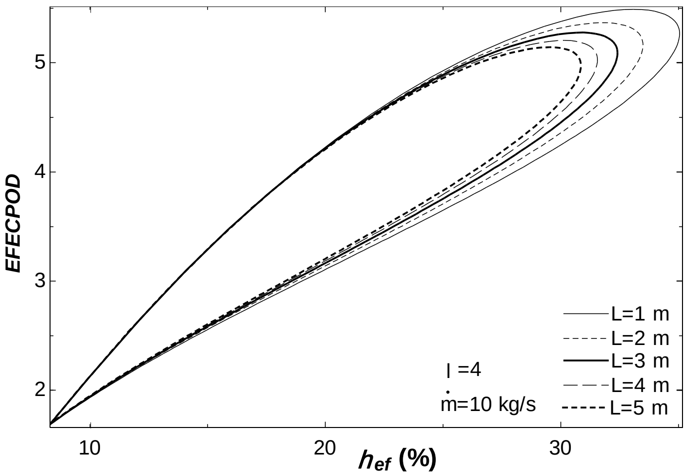

Figure 6. The variation of $EFECPOD$ with respect to η_{ef} at constant λ and $\dot{m}$ for different turbine length

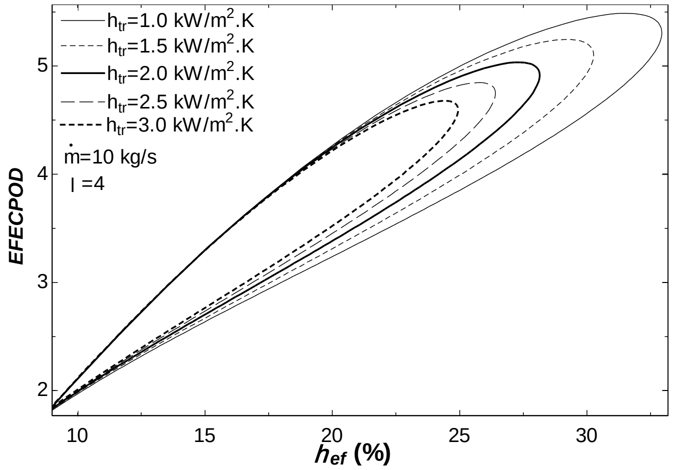

Figure 7. The variation of the $EFECPOD$ with respect to η_{ef} at constant λ and $\dot{m}$ for different heat transfer coefficients

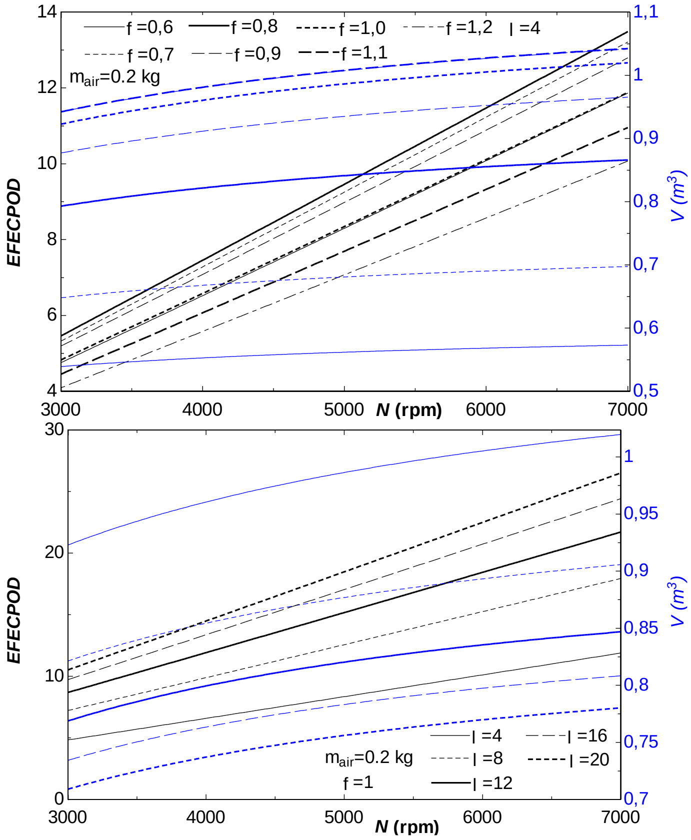

Figure 8. The variation of the $EFECPOD$ with respect to N at constant λ and m_{air} for different ϕ, b) P_{ef} - P_d - $EFECPOD$ with respect to N at constant ϕ and m_{air} for different λ

Figure 7 demonstrates the effects of heat transfer coefficient on the EE and EFECPOD at constant mass flow rate and pressure ratio. As expected, the turbine performance abates with increasing heat transfer coefficient since total heat transfer loss raises.

Figure 8 demonstrates the effects of pressure ratio, equivalence ratio and turbine speed together. It is clear that turbine speed and pressure ratio positively affect the performance parameters. However, there is an optimum point for the equivalence ratio which gives the maximum EFECPOD values. It is approximately 0.8 for the EFECPOD. The turbine performance decreases at higher values of equivalence ratio due to lower combustion

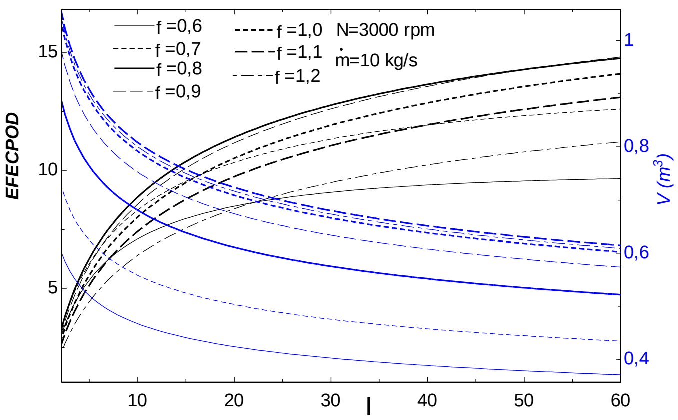

Figure 9. The variation of the $EFECPOD$ with respect to λ at constant N and $\dot{m}$ for different ϕ

efficiency and higher heat transfer and exhaust losses. As can be seen in the figures, the turbine volume is considerably affected by equivalence ratio and pressure ratio. The turbine volume increases with increasing turbine speed and equivalence ratio; decreasing pressure ratio. The maximum turbine volumes are obtained with 4 of the pressure ratio and 1.1 of the equivalence ratio. At the different λ conditions, the maximum combustion temperatures increase and the turbine volumes decreases with increasing pressure ratio. The EFECPOD increases with increasing turbine speed because intake air mass enhances with increasing turbine speed. Another substantial point is that NOx formation is very sensitive the combustion temperatures, thus, it can be said that NOx increases with increasing pressure ratio and turbine speed at the constant ϕ and m_{air} conditions.

Figure 9 demonstrates the effects of equivalence ratio on the turbine performance with respect to changing pressure ratio at constant turbine speed and the mass flow rate of the air. It is obvious that the EFECPOD raise with the enhancing pressure ratio. As similar to previous figures, the optimum points of the equivalence ratios which give the maximum EFECPOD are observed. The maximum value of the EFECPOD increases to a specified value of the equivalence ratio which is 0.8 and then start to decrease. However, the maximum volume is seen at 1.1 of the equivalence ratio.

CONCLUSION

A new performance analysis criterion has been developed and applied to a gas turbine cycle. The effects of the engine design and operating parameters on the performance parameters and energy losses of a gas turbine have been investigated by using the presented analysis criterion. A comprehensive parametrical study has been performed based on numerical examples. In the parametrical studies, the effects of pressure ratio (λ), turbine speed (N), turbine diameter (b), turbine length (L), equivalence ratio (ϕ) and heat transfer coefficient (h_{tr}) on the performance have been examined. The results showed that the determined performance parameter called effective ecological power density (EFECPOD) increases with pressure ratio, turbine speed, turbine diameter; decrease with turbine height (L), heat transfer coefficient (h_{tr}). The EFECPOD increases up to a particular value and then begin to decrease with increasing equivalence ratio. The results are scientifically valuable and therefore, they can be assessed by JBC turbine designers.

NOMENCLATURE

A	heat transfer area (m2)
b	bore (m)
C_v	constant volume specific heat (kJ/kg.K)
C_p	constant pressure specific heat (kJ/kg.K)
F	fuel-air ratio
FTT	finite-time thermodynamics
h_{tr}	heat transfer coefficient (W/ m2K)
H_u	lower heat value of the fuel (kJ/kg)
ICE	Internal combustion engines

l	loss
L	turbine length (m)
m	mass (kg)
$\dot{m}$	time- dependent mass rate (kg/s)
N	engine speed (rpm)
P	pressure (bar), power (kW)
$\dot{Q}$	rate of heat transfer (kW)
r	compression ratio
R	gas constant (kJ/kg.K)
RGF	residual gas fraction
$\bar{S}_P$	mean piston speed (m/s)
T	temperature (K)
v	specific volume (m3/kg)
V	volume (m3)

Greek letters

α	cycle temperature ratio, atomic number of carbon
β	pressure ratio, atomic number of hydrogen
δ	atomic number of nitrogen
ϕ	equivalence ratio
γ	atomic number of oxygen
λ	cycle pressure ratio
ψ	cut-off ratio
ρ	density (kg/m3)
η_C	Isentropic efficiency of compression
η_E	Isentropic efficiency of expansion

Subscripts

1	at the beginning of the compression process
a	air
c	combustion, clearance
cyl	cylinder
ef	effective
f	fuel
ht	heat transfer
i	initial condition
ic	incomplete combustion
in	input
l	loss
max	maximum
me	mean
min	minimum
mix	mixture
out	output
rg	residual gas
s	isentropic condition

sur	surface
st	stoichiometric
t	total
w	cylinder walls

REFERENCES

[1] Zare V, Mahmoudi SMS Yari M. An exergoeconomic investigation of waste heat recovery from the Gas Turbine-Modular Helium Reactor (GT-MHR) employing an ammonia–water power/cooling cycle. Energy. 2013;61: 397–409.

[2] Singh R, Kearney MP and Manzie C. Extremum-seeking control of a supercritical carbon-dioxide closed Brayton cycle in a direct-heated solar thermal power plant. Energy . 2013;60: 380–387.

[3] Singh R, Miller SA, Rowlands AS and Jacobs -PA. Dynamic characteristics of a direct-heated supercritical carbon-dioxide Brayton cycle in a solar thermal power plant. Energy . 2013;50: 194–204.

[4] Abd El-Maksoud RM. Binary Brayton cycle with two isothermal processes. Energy Conversion and Management. 2013;73:303–308.

[5] Singh R, Rowlands AS and Miller SA. Effects of relative volume-ratios on dynamic performance of a direct-heated supercritical carbon-dioxide closed Brayton cycle in a solar-thermal power plant. Energy . 2013;55:1025–1032.

[6] Ferraro V, Imineo F and Marinelli V. An improved model to evaluate thermodynamic solar plants with cylindrical parabolic collectors and air turbine engines in open Joule–Brayton cycle. Energy. 2013;53: 323–331.

[7] Haseli Y. Optimization of a regenerative Brayton cycle by maximization of a newly defined second law efficiency. Energy Conversion and Management. 2013;68: 133–140.

[8] Plaznik U, Tušek J, Kitanovski A and Poredoš A. Numerical and experimental analyses of different magnetic thermodynamic cycles with an active magnetic regenerator. Applied Thermal Engineering. 2013;59(1-2): 52–59.

[9] Malinowski L and Lewandowska M. Analytical model-based energy and exergy analysis of a gas microturbine at part-load operation. Applied Thermal Engineering. 2013;57(1-2): 125–132.

[10] Sim K, Koo B, Kim CH and Kim TH. Development and performance measurement of micro-power pack using micro-gas turbine driven automotive alternators. Applied Energy. 2013;102: 309–319.

[11] Rao AD and Francuz DJ. An evaluation of advanced combined cycles. Applied Energy. 2013;102: 1178–1186.

[12] Ablay G. A modeling and control approach to advanced nuclear power plants with gas turbines. Energy Conversion and Management. 2013;76: 899–909.

[13] Mahto D and Pal S. Thermodynamics and thermo-economic analysis of simple combined cycle with inlet fogging. Applied Thermal Engineering. 2013;51(1-2): 413–424.

[14] Fernández-Villacé V and Paniagua G. On the exergetic effectiveness of combined-cycle engines for high speed propulsion. Energy. 2013;51: 382–394.

[15] Pantaleo AM, Camporeale S and Shah S. Thermo-economic assessment of externally fired micro-gas turbine fired by natural gas and biomass: Applications in Italy. Energy Conversion and Management. 2013;75: 202–213.

[16] Singh OK and Kaushik SC. Thermoeconomic evaluation and optimization of a Brayton–Rankine–Kalina combined triple power cycle. Energy Conversion and Management. 2013;71: 32–42.

[17] Goodarzi M, Kiasat M and Khalilidehkordi E. Performance analysis of a modified regenerative Brayton and inverse Brayton cycle. Energy. 2014;72: 35–43.

[18] Al-Sulaiman FA and K Atif M. Performance comparison of different supercritical carbon dioxide Brayton cycles integrated with a solar power tower. Energy. 2014;72: 35–43.

[19] Le Roux WG, Ochende TB and Meyer JP. The efficiency of an open-cavity tubular solar receiver for a small-scale solar thermal Brayton cycle. Energy Conversion and Management. 2014;84: 457–470.

[20] Dutta P, Kumar P, Ng KC, Murthy SS and Srinivasan K. Organic Brayton Cycles with solid sorption thermal compression for low grade heat utilization. Applied Thermal Engineering. 2014;62(1): 171–175.

[21] Ebrahimi R. Thermodynamic modeling of performance of a Miller cycle with engine speed and variable specific heat ratio of working fluid. Computers and Mathematics with Applications 2011;62: 2169–76.

[22] Ebrahimi R. Performance analysis of an irreversible Miller cycle with considerations of relative air–fuel ratio and stroke length. Applied Math Modeling 2012;36: 4073–9.

[23] Gonca G. Thermodynamic analysis and performance maps for the irreversible Dual–Atkinson cycle engine (DACE) with considerations of temperature-dependent specific heats, heat transfer and friction losses. Energy Convers Manage 2016;111:205–216.

[24] Gonca G, Sahin B. The influences of the engine design and operating parameters on the performance of a turbocharged and steam injected diesel engine running with the Miller cycle. Appl Math Modeling 2016;40(5-6):3764-3782.

[25] Ferguson CR. Internal combustion engines – applied thermosciences. New York: John Wiley & Sons Inc.; 1986.
[26] EES Academic Professional Edition, (2014), V.9.701-3D, USA, F-Chart Software.
[27] Ge Y, Chen L, Sun F, Wu C. Finite-Time Thermodynamic Modelling and Analysis of an Irreversible Otto-Cycle. Appl Energy 2008;85: 618-24.